HEFAT2012
9th International Conference on Heat Transfer, Fluid Mechanics and Thermodynamics
16 – 18 July 2012
Malta

CHARACTERISTICS AND MECHANISM ON CONDENSATE DROP MOVEMENT UNDER BULK SURFACE TEMPERATURE GRADIENT IN MARANGONI DROPWISE CONDENSATION

Zhihao Chen* and Yoshio Utaka
*Author for correspondence
Faculty of Engineering, Yokohama National University,
79-5 Tokiwadai, Hodogaya, Yokohama 240-8501, Japan,
E-mail: zhchen@ynu.ac.jp

ABSTRACT

In Marangoni dropwise condensation, condensate drops move spontaneously when a bulk temperature gradient is applied to the condensing surface. It was considered that the velocity of drop movement is strongly affected by the horizontal component of Marangoni force around a condensate drop. And it is easy to infer that the horizontal component of Marangoni force is decided by both strength of Marangoni force and shape (angle) of condensate drop. In previous studies, it was shown that the velocity of condensate drop movement increases with the increase of bulk surface tension gradient and has a strong relation to initial drop distance. Initial drop distance was adopted as a parameter to express the characteristics of drop velocity, since the qualitatively relations among initial drop distance, Marangoni force and shape of condensate drop inferred from the previous experimental results. However, those relations are still not known clearly in detail. Furthermore, the mechanism on the condensate drop movement is also still not well understood. Therefore, in this paper, experimental study was carried out and the quantitative relation between initial drop distance and angle of condensate drop is investigated. In addition, numerical calculations on the condensation process of water-ethanol vapor mixture and the behavior of condensate were performed by using the VOF (Volume Of Fluid) method to qualitatively analyze the mechanisms of condensate drop movement.

INTRODUCTION

Marangoni dropwise condensation occurs in the condensation of some non-azeotropic mitxtures, such as water-ethanol and water-ammonium mixtures, in which the surface tension of the mixture σ has a negative gradient with the mass fraction of the more volatile component C (so-called 'positive system'). This kind of phenomenon caused by the instability of condensate film due to temperature and surface tension distribution on the condensate liquid. In decades of studing, some researchers such as Mirkovich and Missen [1], Ford and Missen [2] and Fujii [3] et al. carried out experimental studies on Marangoni condensation. As a main determining factor of condensate behavior, the affect of vapor concentration was discussed in these studies. Utaka and Terachi [5,6] measured condensation characteristic curves of water-ethanol vapor and clarified that surface subcooling is one of the dominant factors in determining the condensate and heat transfer characteristics of Marangoni condensation. The mechanisms of Marangoni condensation have also been studied. Hijikata et al. [7] presented a theoretical drop growth mechanism for Marangoni dropwise condensation. They found that the Marangoni effect that occurs due to a difference in the surface tension plays a more important role than the absolute value of the surface tension in Marangoni condensation. Through use of body fitted grid generation method with moving boundaries, Akiyama et al. [8] performed a 2-dimensional numerical simulation for the condensation of water-ethanol vapor on a horizontal heat transfer surface. They found that there's a 2K temperature difference between the condensate film area and crest of condensate drop. As a result of the temperature difference, Marangoni flow occurs in condensate liquid.

Moreover, when a bulk temperature gradient is applied to a horizontal heat transfer surface or in a low-gravity environment under a Marangoni condensation field, condensate drops move spontaneously without any external forces. Since non-uniform temperature distributions are often generated in heat exchangers, it is essential to determine heat transfer to clarify condensate movement in Marangoni condensation when there is a temperature distribution on the heat transfer surface. Moreover, it is possible to control drop movement and heat transfer by generating a temperature distribution on the heat transfer surface. It is believed that this kind of phenomenon could be utilized in some heat transfer device using two-phase flow loop.

In Marangoni dropwise condensation, Marangoni force is induced by the surface tension distribution on condensate surface. The condensate near the periphery of condensate drop was pulled toward the peak along the liquid surface. When a

bulk temperature gradient is applied to heat transfer surface, the Marangoni force acting around the base of a condensate drop become unbalanced and make condensate drops move on the heat transfer surface. This unbalance is thought to be determined by bulk surface tension gradient of condensate. The bulk surface tension gradient here is calculated from the surface tension distribution corresponding to the time-averaged temperature distribution of the thin liquid film covering on the heat transfer surface. In previous study [9], experiments were carried out to investigate the spontaneous movement of condensate drops in Marangoni condensation for water-ethanol vapor mixtures. Movement of condensate drop from low to high temperature side on heat transfer surface was observed. Moreover, although there is a large amount of scatter in drop velocities because the condensate drops coalesce frequently, qualitatively similar tendencies can be observed. Velocity of drop movement increases with the increase of bulk surface tension gradient. However, Chen and Utaka [10] carried out similar experiments in larger range of ethanol mass fraction. They found it is difficult to conclude the characteristics of condensate drop movement only by bulk surface tension gradient. So initial drop distance was adopted as a determining parameter of Marangoni dropwise condensation, and its effect to velocity of drop movement was discussed in the study. As a result, unambiguous relations between average drop velocity and bulk surface tension gradient/initial drop distance were elucidated. However, the reason for adopting initial drop distance as the dominant parameter here is the inferred correspondence correlations among initial drop distance, Marangoni force and shape of condensate drop based on the previous experimental results [11, 12]. The quantitative correlations among the three factors above are still not well understood.

The objective of this study is to confirm the quantitative correlations among initial drop distance, Marangoni force and shape of condensate drop. In particular, initial drop distance and angle of condensate drop were measured and their quantitative relation was discussed. Furthermore, a qualitatively discussion on the 3-dimensional phenomenon of drop movement in Marangoni condensation was carried out by performing a 2-dimensional numerical simulation using VOF method. The mechanism on condensate drop movement in Marangoni dropwise condensation was discussed.

NOMENCLATURE

C		Mass fraction of ethanol vapor
C_P	[J/kg·K]	Specific heat at constant pressure
D	[m^2/s]	Diffusion coefficient
F		VOF function, Marangoni force
g	[m/s^2]	Gravity acceleration
Δh	[kJ/kg]	Latent heat
M	[N·s]	Momentum
$\dot{m}$	[kg/m^2·s]	Mass flux of condensation
P	[kPa]	Pressure
T	[K]	Temperature
ΔT	[K]	Surface subcooling
t	[s]	Time
u	[m/s]	Horizontal velocity
v	[m/s]	Vertical velocity
x	[m]	Cartesian axis direction
y	[m]	Cartesian axis direction

Greek characters

θ	[°]	Angle of condensate drop
σ	[mN/m]	Surface tension coefficient
λ	[W/m·K]	Thermal conductivity
υ	[m^2/s]	Kinematic viscosity
ρ	[kg/m^3]	Density
τ	[Pa]	Shear stress

Subscripts

a	Advancing angle
r	Receding angle
surf	Vapor-liquid interface
E	Ethanol
L	Liquid phase, low temperature side
V	Vapor phase
H	High temperature side
x	horizontal

PREVIOUS RESULTS AND THE RELATIONS TO THIS STUDY

Around the periphery of condensate drops, condensate is pulled into condensate drops by Marangoni force. So the condensate drops experience a reactive force of Marangoni force as shown in Figure 1. When a bulk temperature gradient applied on heat transfer surface, the reactive force around a condensate drop become unbalanced and condensate drops move towards the high temperature side. Because the shape (angle) of condensate drops changes with the variation of Marangoni force, the horizontal component of Marangoni force changes with both Marangoni force and angle of condensate

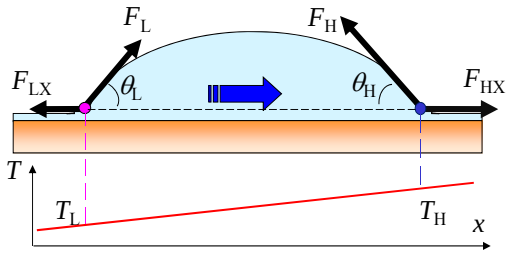

Figure 1 Schematic diagram of driving force for condensate drop movement

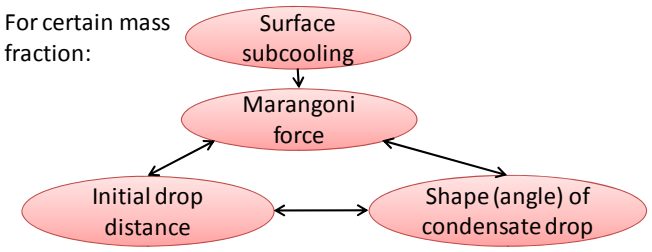

Figure 2 Correlations between Marangoni force, initial drop distance and condensate drop shape

drop, it is easy to consider that the velocity of condensate drop is also affected by the two factors. In previous study [10], initial drop distance was adopted as a dominant parameter which represents Marangoni force and angle of condensate drop. As shown in Figure 2, there are correspondence relations among Marangoni force, initial drop distance and angle of condensate drop. Those correspondence relations were inferred based on the previous experimental results. That is, with the decreasing of initial drop distance the thin liquid film existing between condensate drop becoming thinner and the heat transfer coefficient getting higher (indicating more amount of condensate). Among the three factors, Marangoni force is impossible to measure, angle of condensate drop has large amount of scatter because of frequent coalescence of condensate drops. Different with the two factors, initial drops grow from a thin flat condensate film that appears immediately after a drop departs, the state before the drops form is relatively stable. So the measurement of initial drop distance has good repeatability. As an example, the results of ethanol mass fraction C=0.15 was shown in Figure 3. When the initial drop distance decreases, the average drop velocity initially increases and then decreases after reaching a maximum value at almost the same surface tension gradient. Moreover, as shown in Figure 4, the drop velocity increases linearly with increasing bulk surface tension gradient for each initial drop distance range. The gradient of the lines increases with increasing initial drop distance.

In summary, although qualitatively similar tendencies between drop velocity and bulk surface tension gradient/initial drop distance can be observed in the experimental results, the quantitative relations among initial drop distance, Marangoni force and angle of condensate drop are still not well understood. So in this study, experimental studies were carried out to confirm the inferred correlations among initial drop distance, angle of condensate drop and Marangoni force.

EXPERIMENTAL APPARATUS AND METHOD

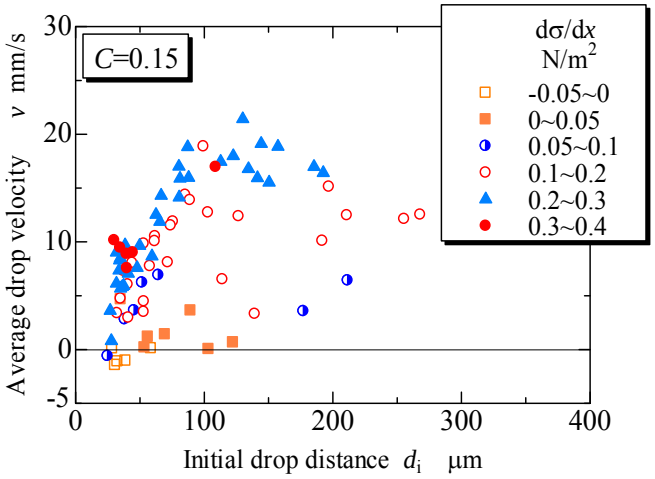

Figure 3 Variation of condensate drop velocity against initial drop distance for C=0.15

Figure 5 shows a schematic of the condensing chamber. A vapor mixture was generated by electrically heating a water-ethanol mixture with a certain mass fraction in a vapor generator. The vapor was conducted into the condensing chamber and partially condensed on the heat transfer block, and it was almost completely condensed in the auxiliary condenser after passing through the condensing chamber. The vapor pressure was maintained close to atmospheric pressure by a small opening to the atmosphere between the auxiliary condenser and the condensate receiver. The condensate was fed back into the vapor generator after deaeration, which was used to remove non-condensable gas dissolved in the condensate.

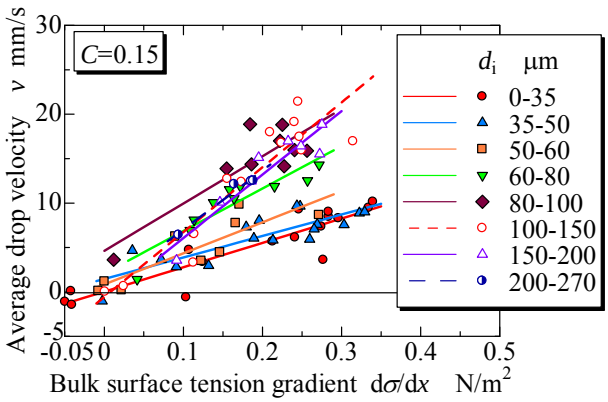

Figure 4 Variation of condensate drop velocity against bulk surface tension gradient for C=0.15

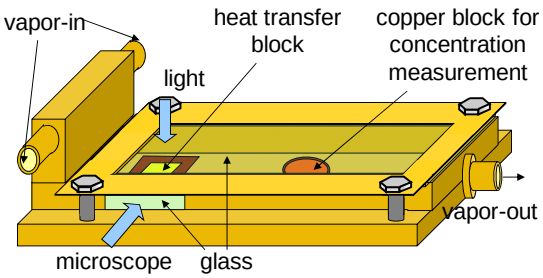

Figure 5 Condensing chamber

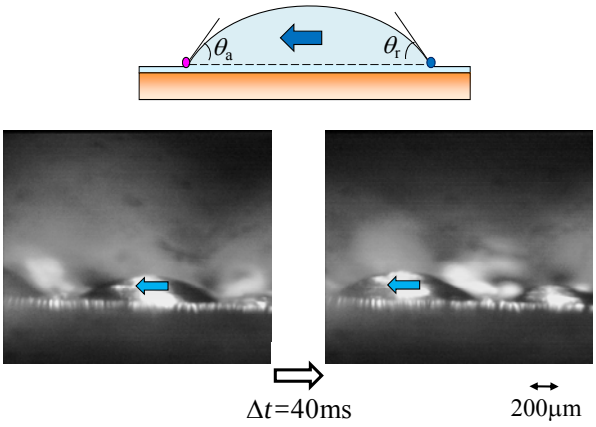

Figure 6 Aspect of condensate drop shape

The heat transfer block was made of brass with a surface area of 20 × 20 mm^2 and a thickness of 6.7 mm, a heat-resistant material made of constantan with a triangular cross-section was soldered onto the cooling surface of the heat transfer block. This allowed a bulk temperature gradient to be applied to the heat transfer surface by uniformly cooling the heat-resistant material. Two windows for observation were set on the condensing chamber as shown in figure 5. The movement and shape of condensate drops could be observed through the two windows. For temperature measurement, 16 T-type sheathed thermocouples of 0.5mm in diameter were set in the heat transfer block. So the temperature distribution and heat transfer coefficient on heat transfer surface could be calculated based on the measured temperature distribution in the heat transfer block.

In addition, to distinguish the driving force of drop movement from the shearing force of vapor flow, the vapor was made to flow in the opposite direction to the condensate drop movement.

The velocity of drop movement, initial drop distance and angle of condensate drop were measured from the images shot through a microscope with high-speed camera. In order to analyze the uncertainties of these measurements, continuous measurement over 10 times by using a same image file were carried out. Then, the average value of the measured results was calculated. The maximum deviation from the average value for each measured result was discussed. As a result, the uncertainty of drop velocity, the initial drop distance and the angle of condensate drop is about 0.2mm/s, 0.35μm and 1.5°, respectively. For the experimental results, drop velocity is in the range of 0~50mm/s, initial drop distance and the angle of condensate drop are in the range of 0~300μm, 0~50°, respectively. It is obvious that the uncertainties of these measurements are quite small compared to the experimental results. Moreover, the thermocouples embedded in the heat transfer block are carefully calibrated that brought down their uncertainties to less than ±0.05 K, together with the location bias of the thermocouples, a ±0.20K uncertainty of the temperature of condensing surface is induced.

EXPERIMENTAL RESULTS AND DISCUSSION

(a) Angle of condensate drop

The angle of condensate drop was measured in relative low range of ethanol mass fractions (C=0.05, 0.10, 0.15, 0.20). The profile image of a condensate drop taken through the side view window was shown in figure 6. Vapor flows into from the left side of the photo, and the left side is the high temperature side of heat transfer surface. So the condensate drop moves from the right side to left side as shown in figure 6. Here the angle between surface of condensate drop and heat transfer surface near the drop base as shown in the schematic in figure 6 is defined as angle of condensate drop. Moreover, the angle in the direction of forward movement is named 'advancing angle θ_a' and the other one at the opposite side is named 'receding angle θ_r'.

The variations of advancing and receding angles against surface subcooling are shown in figure 7. For relative small surface subcooling (the corresponding heat transfer coefficient is less than its maximum value), similar tendencies could be seen on the advancing and receding angles: both the advancing and receding angles increase with the increase of surface subcooling. In addition, the angles are in the range of about 10°~50°. Similar to the velocity of drop movement, it is also could be seen that there are a large amount scatter in the angle of condensate drop. As mentioned above, it is caused by the frequent coalescence when the drops are moving or the variation of temperature distribution on the heat transfer surface. The wild scatter is considered to be an essential characteristic of Marangoni dropwise condensation.

(b) Relation between initial drop distance and angle of condensate drop

As stated above, similar tendencies could be seen on the variation of advancing and receding angles. So the average value of the advancing and receding angle angle of single condensate drop was calculated and the relations among average angle of condensate drop, initial drop distance and the heat transfer coefficient are discussed.

The variations of average angle of condensate drop, initial drop distance and heat transfer coefficient against surface subcooling are shown in figure 8. Several tendencies could be seen in the figure. In each mass fraction of ethanol, same with the previous results, heat transfer coefficient increases with the increase of surface subcooling and initial drop distance decreases. In addition, the average angle of condensate drop increases with the increasing surface subcooling. This means that the decreasing initial drop distance corresponds to the increasing angle of condensate drop. The maximum of average angle of condensate drop is about 35°~45°, which is a little bit smaller than the typical contact angle of condensate drop on hydrophobic surface. Moreover, for same value of surface subcooling, higher heat transfer coefficient and the corresponding smaller initial drop distance was realized in the condition of smaller mass fraction of ethanol.

From the experimental results above, it is believed that in the condition of larger surface subcooling or lower mass fraction of ethanol, initial drop distance has smaller value but average angle of condensate drop shows larger value because of the stronger Marangoni force. It could be confirmed here that the three factors shown in figure 2 have the quantitative correspondent relations. It is suitable for adopting initial drop distance as the dominant parameter of Marangoni dropwise condensation that representing the Marangoni force and shape of condensate drop in the previous studies.

ABOUT THE MECHANISM ON CONDENSATE DROP MOVEMENT

So far, experimental studies on characteristics of drop movement (effects of some parameters) have been carried out under a bulk temperature gradient on heat transfer surface in Marangoni dropwise condensation of water-ethanol vapor. However, it is impossible to measure the Marangoni force which is considered to be deeply related to the driving force of drop movement. So in order to investigate the mechanism on the drop movement, a numerical simulation was carried out by

using the VOF method. Because this 3-dimensional phenomenon was simulated by a 2-dimensional calculation in the calculation region shown in figure 9, only qualitative discussion only qualitative discussion was performed in this paper.

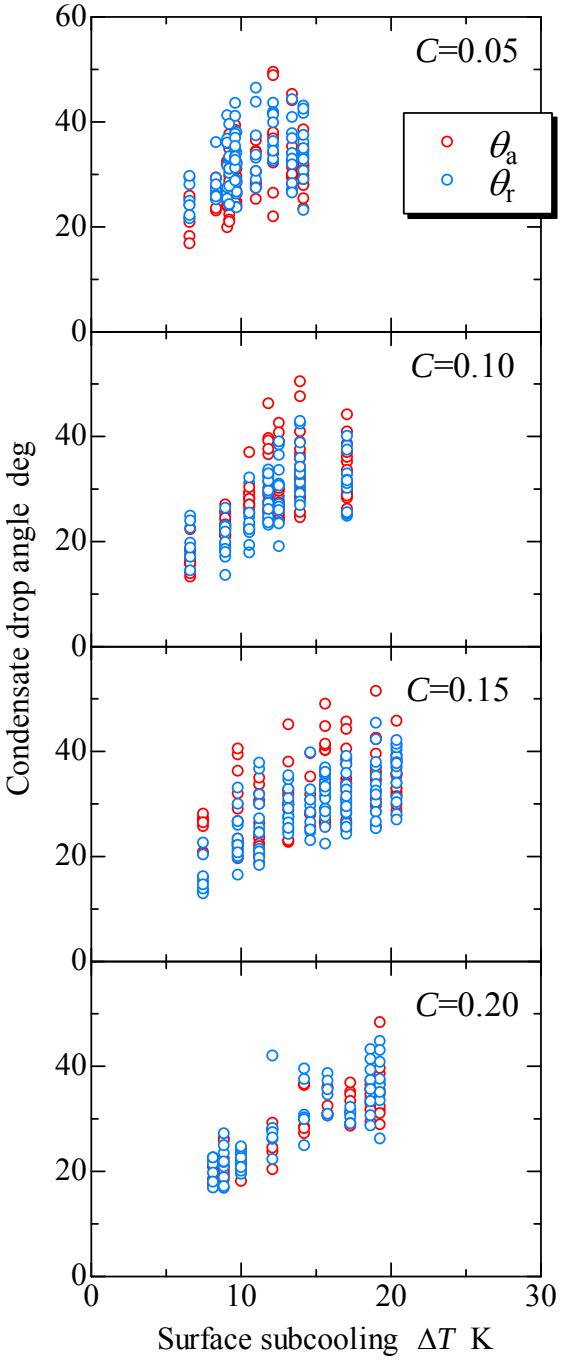

Figure 7 Variations of advancing and receding angle (θ_a and θ_r) of condensate drops

BASIC EQUATIONS

(a) Liquid phase

$$\frac{\partial u_L}{\partial x}+\frac{\partial v_L}{\partial y}=0 \tag{1}$$

$$\frac{\partial u_L}{\partial t}+u_L\frac{\partial u_L}{\partial x}+v_L\frac{\partial u_L}{\partial y}=g_x-\frac{1}{\rho_L}\frac{\partial P}{\partial x}+\upsilon_L\left(\frac{\partial^2 u_L}{\partial x^2}+\frac{\partial^2 u_L}{\partial y^2}\right) \tag{2}$$

$$\frac{\partial v_L}{\partial t}+u_L\frac{\partial v_L}{\partial x}+v_L\frac{\partial v_L}{\partial y}=g_y-\frac{1}{\rho_L}\frac{\partial P}{\partial y}+\upsilon_L\left(\frac{\partial^2 v_L}{\partial x^2}+\frac{\partial^2 v_L}{\partial y^2}\right) \tag{3}$$

$$\frac{\partial T_L}{\partial t}+u_L\frac{\partial T_L}{\partial x}+v_L\frac{\partial T_L}{\partial y}=\frac{\lambda_L}{\rho_L C_{P,L}}\left(\frac{\partial^2 T_L}{\partial x^2}+\frac{\partial^2 T_L}{\partial y^2}\right) \tag{4}$$

$$\frac{\partial C_L}{\partial t}+u_L\frac{\partial C_L}{\partial x}+v_L\frac{\partial C_L}{\partial y}=D_L\left(\frac{\partial^2 C_L}{\partial x^2}+\frac{\partial^2 C_L}{\partial y^2}\right) \tag{5}$$

$$\frac{\partial F}{\partial t}+\frac{\partial u_L F}{\partial x}+\frac{\partial v_L F}{\partial y}=0 \tag{6}$$

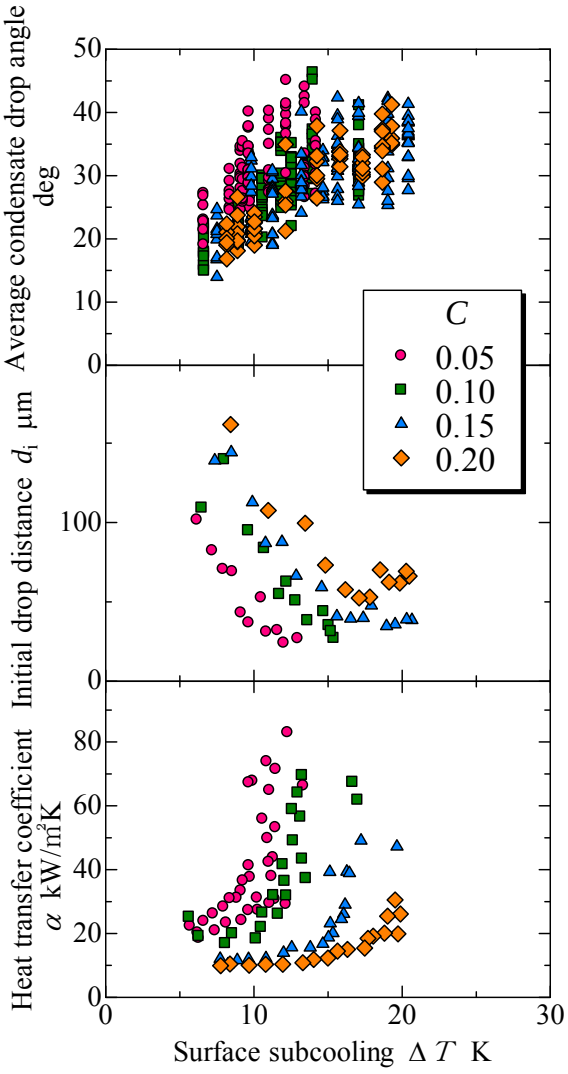

Figure 8 Variations of condensate drop shape, initial drop distance and heat transfer coefficient against surface subcooling

In the calculation, the liquid phase was treated as incompressible. The continuity equation, momentum equation and energy equation were solved.

(b) Vapor phase

In the vapor phase, the vapor velocity in *y*-direction was assigned by the condensate rate at the vapor-liquid interface, and the vapor velocity in *x*-direction was ignored. The diffusion equation was solved based on the assigned vapor velocity. After getting the calculation results of diffusion equation, the temperature of vapor mixture was calculated from the mass fraction distribution based on the vapor-liquid equilibrium under the assumption of saturated state.

$$\rho_V v_V = \dot{m} \tag{7}$$

$$\frac{\partial C_V}{\partial t} + v_V \frac{\partial C_V}{\partial y} = D_V \left(\frac{\partial^2 C_V}{\partial x^2} + \frac{\partial^2 C_V}{\partial y^2} \right) \tag{8}$$

$$T_V = f\left(C_V\right) \tag{9}$$

(c) Vapor-liquid interface

The velocity distribution at vapor-liquid interface is calculated by taking account of the effect of surface tension gradient (stress balance at the vapor-liquid interface).

The velocity distribution at vapor-liquid interfacial was used as the boundary condition of liquid phase. At the interface, temperature and mass fraction was calculated based on the vapor-liquid equilibrium, energy balance and mass balance.

Condensation rate

$$\rho_V v_V = \dot{m} \tag{10}$$

Energy balance

$$-\lambda_L \frac{\partial T_L}{\partial y} = \Delta h_V \dot{m} \tag{11}$$

Mass balance

$$\dot{m}_E = \rho_V D_V \frac{\partial C_V}{\partial y} + C_V \dot{m} \tag{12}$$

Mass fraction of liquid in the cell at the interface

$$C_L = \frac{\dot{m}_E}{\dot{m}} \tag{13}$$

Vapor-liquid equilibrium

$$C_V = f\left(T_{surf}\right) \tag{14}$$

$$C_L = f\left(T_{surf}\right) \tag{15}$$

Relation of surface tension coefficient and concentration of liquid

$$\sigma = f\left(C_L\right) \tag{16}$$

Increase of *F* caused by the condensation

$$\frac{\partial F}{\partial t} = \frac{1}{\rho_L} \frac{\dot{m}}{\Delta y} \tag{17}$$

Stress balance at the vapor-liquid interface

$$\left(P_V - P_L + \frac{\sigma}{R} \right) n_i = \left(-\tau_{L,ij} \right) n_k + \frac{\partial \sigma}{\partial x_i} \tag{18}$$

BOUNDARY CONDITIONS AND INITIAL CONDITIONS

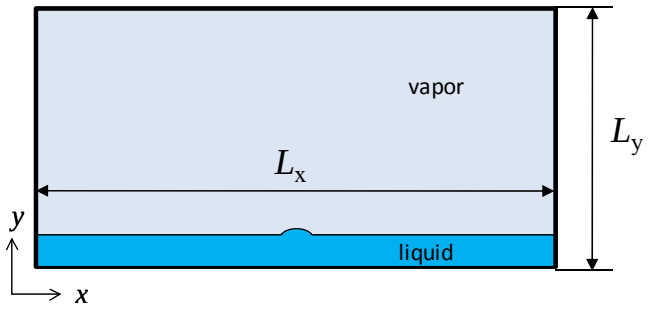

Figure 9 Calculation domain

Considering the real phenomenon and the computation time, the calculation is carried out in a relative small region of 600μm×200μm as shown in figure 9. The boundary y=0 is set as the condensing surface, and y=L_y is the steady temperature/concentration boundary. In addition, boundary condition at x=0, L_x is the free inlet/outlet flow. A thin liquid film of 1.5μm in thickness is set initially on the condensing surface. A tiny protuberance is also given in the center of the initial liquid film as a disturbance. During the calculation, certain mass fraction of ethanol vapor and the corresponding vapor line temperature are assigned to the boundary of y=L_y, temperature gradient (the right side was set as the high temperature side) was assigned directly to the condensing surface of y=0. During the calculation a constant temperature was initially assigned to the condensing surface. After the temperature/concentration distribution in the calculation region got closed to the real phenomenon with time elapses, the temperature gradient was applied to the condensing surface.

Furthermore, the basic equations were discretized by the use of a staggered grid. Convective term was approximated by 1-order upwind difference and diffusion term by 2-order central difference. Pressure was solved implicitly. And other variables such as velocity, temperature and mass fraction were solved explicitly. The velocity field in the calculation region was calculated using the SOLA method (HSMAC method). In addition, the variations of *F* at the vapor-liquid interface were calculated by using the donor-acceptor method.

CALCULATION RESULTS AND DISCUSSIONS

(a) Variation of liquid film and shape of condensate drop

The calculation results for ethanol mass fraction of 0.09 were shown in figure 10~13. The variations in thickness of condensate film and form of free surface were shown in figure 10. The condensate film was getting thicker as time passes. There were several condensate drops forming and then getting larger on the condensing surface including on the spot where the initial disturbance was given. The condensate drops here are similar with those that formed in the experiments.

(b) Discussion on the angle of condensate drop

As shown in figure 11, the condensate drops forming on the condensing surface were compared for difference surface

subcoolings (ΔT=6K and 10K). The condensate drops that are close in diameter were selected and the shape of the drops was compared here. Moreover, the developed condensate drops were investigated here in order to avoid the influence of initial conditions. As shown in figure 11, the top of condensate drop was higher when the surface subcooling ΔT is larger (10K). It means that angle of condensate drop becomes larger when the surface subcooling is bigger. This is coincident to the experimental results, and indicates the angle of condensate drop become larger because of the stronger Marangoni force.

(c) Discussion on the driving force of drop movement

In order to investigate the relation between condensate drop movement and Marangoni force around periphery of condensate drops which is considered to be related to the driving force of drop movement, the momentum of condensate liquid which is pulled into condensate drop by Marangoni force were calculated. In this 2-dimensional simulation, the momentum on the high and low temperature side of a condensate drop was calculated and the qualitative relation between the movement of condensate drop and the unbalance of momentum in horizontal direction was discussed. In addition, the momentum was calculated on the position where condensate film around the periphery of condensate drop is the thinnest (in the valley around base of condensate drop).

So far, from the experimental results, it was known that there were a large amount of scatter in the velocities and angles of condensate drop because of the coalescence of drops or unstable temperature distribution near the periphery of drops. Similar to the experimental results, it is thought that the properties of condensate drop vary greatly around the average

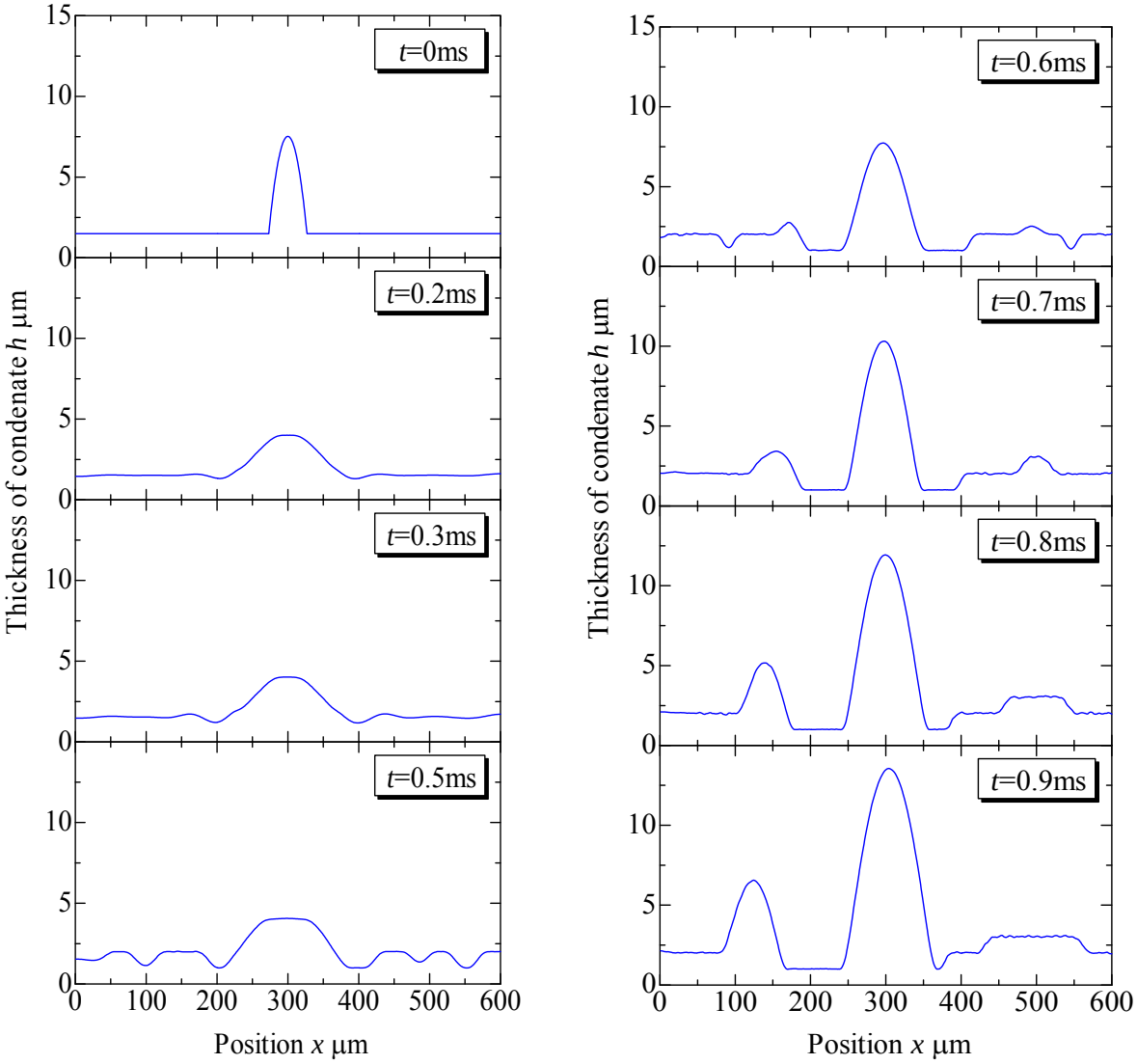

Figure 10 Variation of thickness of condensate liquid film (C=0.09, ΔT=6K)

values in the numerical simulation. So in order to avoid the influence of adjacent condensate drops, the momentum of relatively isolated condensate drop which is believed to be close to the mean state of condensate drops was calculated in the numerical simulation. In this study, the condensate drop formed at the center of condensing surface as shown in figure 10 was selected.

For C=0.09, ΔT=10K, the behavior of growing condensate drop after the temperature gradient was applied to heat transfer surface is shown in figure 12. Symbol ○ in the figure denotes the crest of condensate drops. In addition, the horizontal component of momentum at high/low temperature side of condensate drop and the temperature difference of liquid surface between high and low temperature side were shown in (a) and (b) of figure 13, respectively. The high/low temperature side here means the high/low temperature side of the condensing surface which is set as the boundary condition. That is, the right side is the high temperature side and the left side is the low temperature side. As shown in figure 13, surface temperature of condensate on the right side is higher than that of the left side. And the horizontal momentum of condensate liquid on the right side (high temperature side) is larger than that of the left side. Corresponding to these results, as shown in figure 12, it could be seen that condensate drop moves towards the right side when it is growing. In conclusion, the direction of condensate drop movement is coincident with the side of larger momentum of condensate liquid being pulled into drop by Marangoni force. So it could be inferred that the unbalance of horizontal component of Marangoni force is the driving force of condensate drop movement.

CONCLUSION

In this study, experimental and numerical investigations on the characteristics and mechanism of condensate drop movement in Marangon dropwise condensation of water-ethanol vapor mixture were carried out. The following conclusions may be drawn from the results.

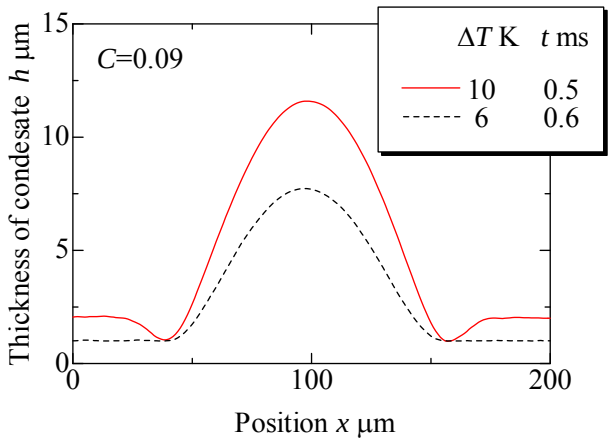

Figure 11 Comparison of condensate drop shape for different subcooling (C=0.09)

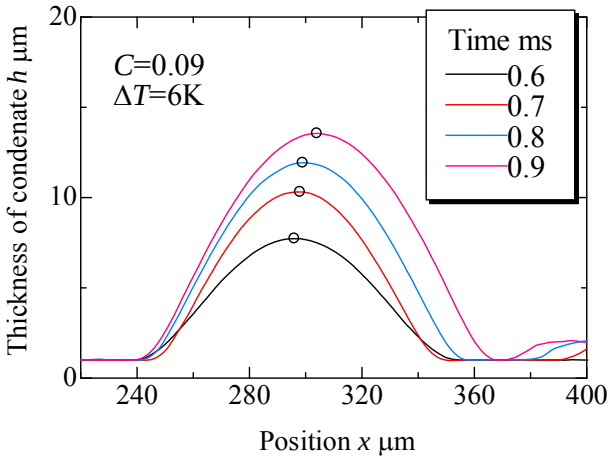

Figure 12 Growth and movement of a condensate drop (C=0.09, ΔT=6K)

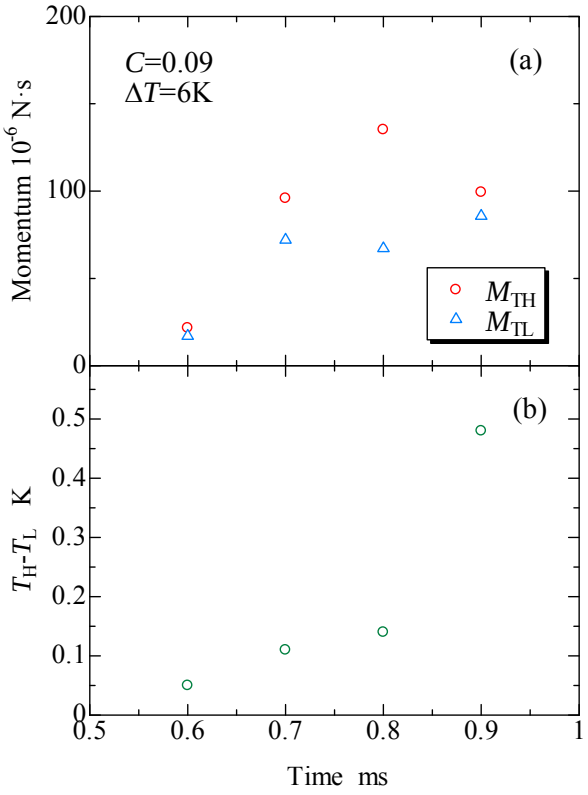

Figure 13 (a) Horizontal momentum of condensate liquid being driven into a condensate drop (b) Surface temperature difference between low and high temperature side of a condensate drop

(1) It is believed that there is deep relation between Marangoni force and angle of condensate drop. As both confirmed by the results of experiments and numerical simulations, the angle of condensate drop is larger when the Marangoni force is stronger (surface subcooling of the condensing surface is larger).

(2) Correspondent relation exists between initial drop distance and angle of condensate drop. Base on the experimental results, with the increase of surface subcooling, initial drop distance decreases, angle of condensate drop increases and heat transfer coefficient increases. From these corresponding relations, it could be confirmed that it was suitable for adopting initial drop distance as the dominant parameter representing the Marangoni force and shape of condensate drop in the previous studies.

(3) In the numerical simulation, condensate liquid around the periphery of condensate drop is pulled into the drop by Marangoni force. It was confirmed that the condensate drop moves towards the side on which the momentum of liquid being pulled into condensate drop is larger. So it could be inferred that the unbalance of horizontal component of Marangoni force is the driving force of condensate drop movement.

REFERENCES

[1] Mirkovich, V.V. and Missen, R.W., Non-Filmwise Condensation of Binary Vapor of Miscible Liquids, *The Canadian Journal of Chemical Engineering*, Vol. 39 (1961), pp. 86-87.

[2] Ford, J.D. and Missen, R.W., On the Conditions for Stability of Falling Films Subject to Surface Tension Disturbances; the Condensation of Binary Vapor, *The Canadian Journal of Chemical Engineering*, Vol. 48 (1968), pp. 309-312.

[3] Fujii, T., Koyama, S., Simizu, Y., Watabe, M. and Nakamura, Y., Gravity Controlled Condensation of an Ethanol and Water Mixture on a Horizontal Tube, *Transactions of JSME (B)*, Vol. 55, No. 509 (1989), pp. 210-215.

[4] Utaka, Y. and Terachi, N., Measurement of Condensation Characteristic Curves for Binary Mixture of Steam and Ethanol Vapor, *Heat Transfer-Japanese Research*, Vol. 24, No. 1 (1996), pp. 57-67.

[5] Utaka, Y. and Terachi, N., Study on condensation heat transfer for steam-ethanol vapor mixture (Relation between condensation characteristic curve and modes of condensate), *Transactions of the JSME*, *Series B*, Vol. 61, No. 588 (1995), pp. 3059-3065.

[6] Utaka, Y. and Wang, S., Characteristic Curves and the Promotion Effect of Ethanol Addition on Steam Condensation Heat Transfer, *International Journal of Heat and Mass Transfer*, Vol. 47 (2004), pp. 4507-4516.

[7] Hijikata, K., Fukasaku, Y. and Nakabeppu, O., Theoretical and Experimental Studies on the Pseudo-Dropwise Condensation of a Binary Vapor Mixture, *Journal of Heat T*ransfer, Vol. 118 (1996), pp. 140-147.

[8] Akiyama, H., Nagasaki, T. and Ito, Y., A Study on the Mechanism of Dropwise Condensation in Water-Ethanol Vapor Mixture, *Thermal Science & Engineering*, Vol. 9, No. 6 (2001), pp. 19-27.

[9] Utaka, Y. and Kamiyama, T., Condensate Drop Movement in Marangoni Condensation by Applying Bulk Temperature Gradient on Heat Transfer Surface, *Heat Transfer-Asian Research*, Vol. 37, No. 7 (2008), pp. 387-397.

[10] Chen, Z. and Utaka, Y., Drop Movement under Bulk Temperature Gradient of Heat Transfer Surface in Marangoni Dropwise Condensation (Effect of Initial Drop Distance), *Transactions of JSME (B)*, Vol. 75, No. 757 (2009), pp. 90-97.

[11] Utaka, Y., Kenmotsu, T. and Yokoyama, S., On Condensation Heat Transfer for Water and Ethanol Vapor Mixture (Observation of Drop Formation and Departure Processes for Marangoni Dropwise Condensation), *Transactions of the JSME*, *Series B*, Vol. 64, No. 626 (1998), pp. 3364-3370.

[12] Utaka, Y. and Nishikawa, T., Measurement of Condensate Film Thickness for Solutal Marangoni Condensation Applying Laser Extinction Method, *Journal of Enhanced Heat Transfer*, Vol. 10, No. 1 (2003), pp. 119-129.